Editorial

11th International GeoRaman Conference (pages 807–809)
Craig P. Marshall
Article first published online: 11 SEP 2015 | DOI: 10.1002/jrs.4783

Research articles

Autonomous soil analysis by the Mars Micro-beam Raman Spectrometer (MMRS) on-board a rover in the Atacama Desert: a terrestrial test for planetary exploration (pages 810–821)
Jie Wei, Alian Wang, James L. Lambert, David Wettergreen, Nathalie Cabrol, Kimberley Warren-Rhodes and Kris Zacny
Article first published online: 9 FEB 2015 | DOI: 10.1002/jrs.4656

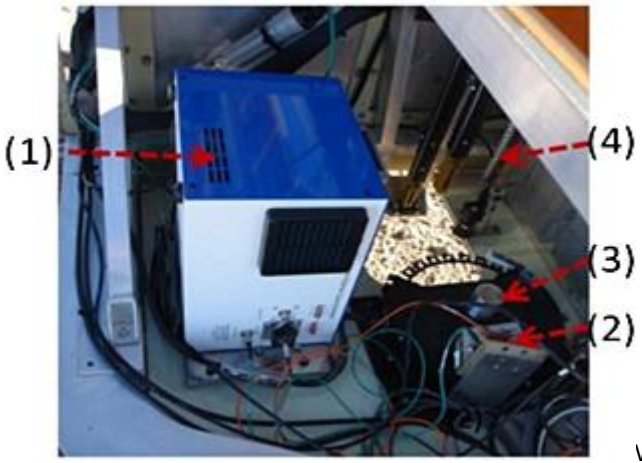

We report the first rover test of the Mars Micro-beam Raman Spectrometer (CW 532 nm), developed for flight in the Atacama Desert. The spectrometer was integrated on a rover and analyzed subsurface soil samples brought up by a 1-m drill and delivered by a carousel. The spectrometer demonstrated robust performance over 50-km traverse on rugged terrains and in a challenging environment. Igneous minerals, carbonates, sulfates and carbonaceous materials were unambiguously identified. Quantified distributions of major minerals and carbonaceous materials are extracted.

Reference Raman spectra of synthesized $CaCl_2 \cdot nH_2O$ solids ($n = 0, 2, 4, 6$) (pages 822–828)
Lucas M. Uriarte, Jean Dubessy, Pascal Boulet, Valentin G. Baonza, Isabelle Bihannic and Pascal Robert
Article first published online: 9 JUN 2015 | DOI: 10.1002/jrs.4730

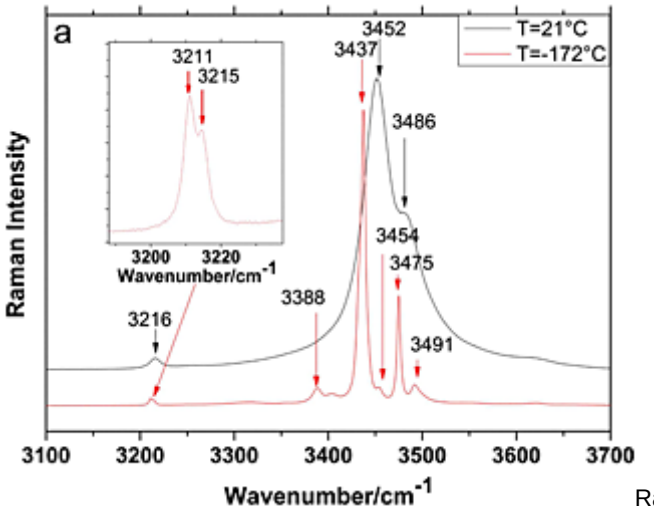

Raman spectra of $CaCl_2 \cdot nH_2O$ ($n = 0, 2, 4, 6$) solids

unambiguously identified by X-ray diffraction (XRD) are given in the spectral range 100–4000 cm^{-1} at room temperature and −172 °C. Band assignment is discussed over the whole spectral range. These new data are reference spectra for geochemical and planetology exploration. An original method of synthesis of these solids in capillary is validated and allows their study by both XRD and Raman spectroscopy.

Understanding the Raman spectral features of phyllosilicates (pages 829–845)
Alian Wang, John J. Freeman and Bradley L. Jolliff
Article first published online: 14 APR 2015 | DOI: 10.1002/jrs.4680

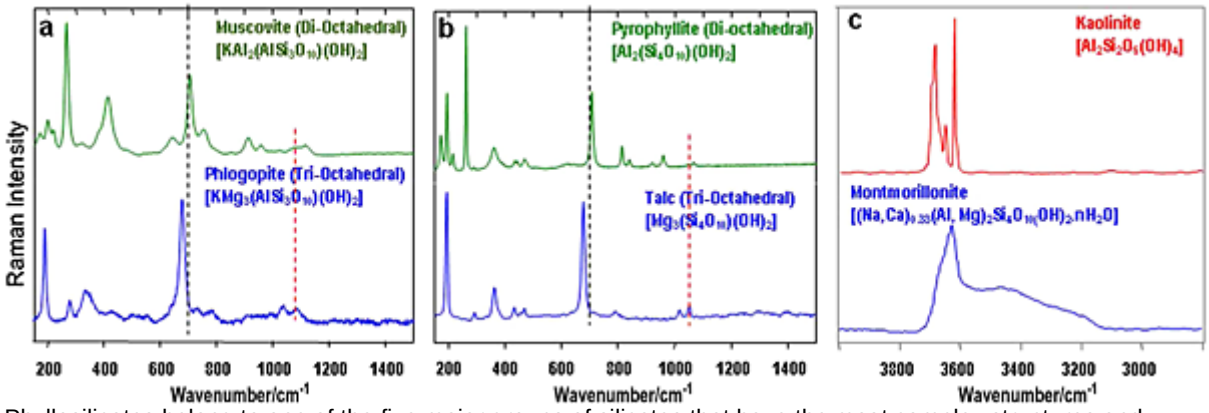

Phyllosilicates belong to one of the five major groups of silicates that have the most complex structures and chemistry. However, phyllosilicates were found at Mars surface by X-ray diffraction and Vis-Near IR spectroscopy though *in situ* surface exploration and orbital remote sensing. This study presents the first systematic Raman spectroscopic study on five major groups of phyllosilicates, which build a foundation for phyllosilicate characterization on Mars and other planetary bodies in our Solar System by *in situ* Raman spectroscopy.

Raman, FTIR and XRD study of Icelandic tephra minerals: implications for Mars (pages 846–855)
FREE
Emily J. Bathgate, Helen E. Maynard-Casely, Graziella Caprarelli, Linda Xiao, Barbara Stuart, Kate T. Smith and Ross Pogson
Article first published online: 27 APR 2015 | DOI: 10.1002/jrs.4694

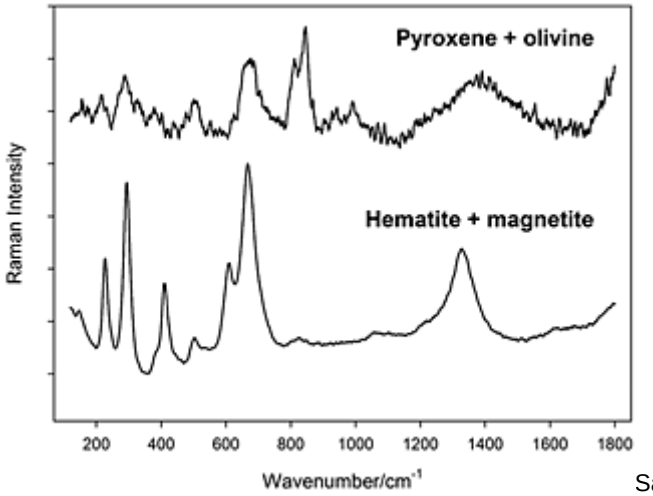

Samples of tephra from two Icelandic volcanoes were prepared and analysed by Raman spectroscopy, XRD and FTIR spectroscopy. The results are discussed in the context of relative success of the techniques in identifying primary and secondary minerals of volcanic products. This is relevant to the future exploration of planet Mars.

Raman spectroscopy for future planetary exploration: photodegradation, self-absorption and quantification of carotenoids in microorganisms and mineral matrices (pages 856–862)
Jan-Hein Hooijschuur, Mattheus F.C. Verkaaik, Gareth R. Davies and Freek Ariese

Article first published online: 15 JAN 2015 | DOI: 10.1002/jrs.4647

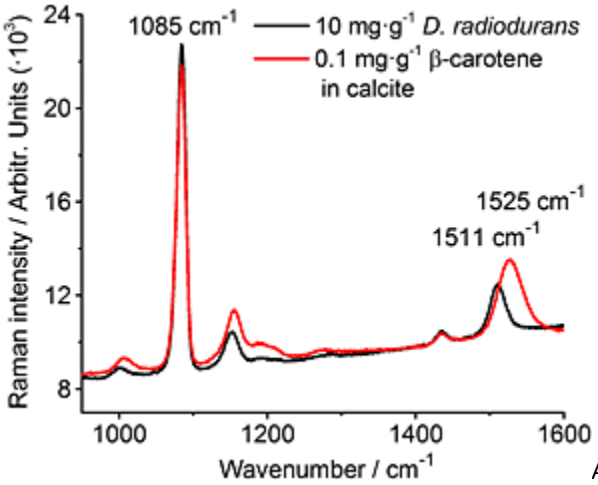

At resonance Raman conditions, low concentrations of biomarkers can be detected, but photodegradation and self-absorption effects need to be taken into account. We show a semi-quantitative analysis of the carotenoid content of extremophile bacteria in a calcite matrix.

Avoiding misidentification of bands in planetary Raman spectra (pages 863–872)

Liam V. Harris, Melissa McHugh, Ian B. Hutchinson, Richard Ingley, Cédric Malherbe, John Parnell, Alison Olcott Marshall and Howell G. M. Edwards

Article first published online: 4 MAR 2015 | DOI: 10.1002/jrs.4667

Raman spectra of several terrestrial Mars analogue samples, representative of a range of aspects of Martian geology, are used to illustrate potential sources of ambiguity or confusion, which may arise when analysing Raman spectra returned by future planetary exploration missions. We recommend the minimum operating parameters that should be considered for flight spectrometers, capable of unambiguous differentiation between the mineral and molecular targets presented here.

Revealing the biotic origin of silicified Precambrian carbonaceous microstructures using Raman spectroscopic mapping, a potential method for the detection of microfossils on Mars (pages 873–879)
Frédéric Foucher, Mohamed-Ramzi Ammar and Frances Westall
Article first published online: 14 APR 2015 | DOI: 10.1002/jrs.4687

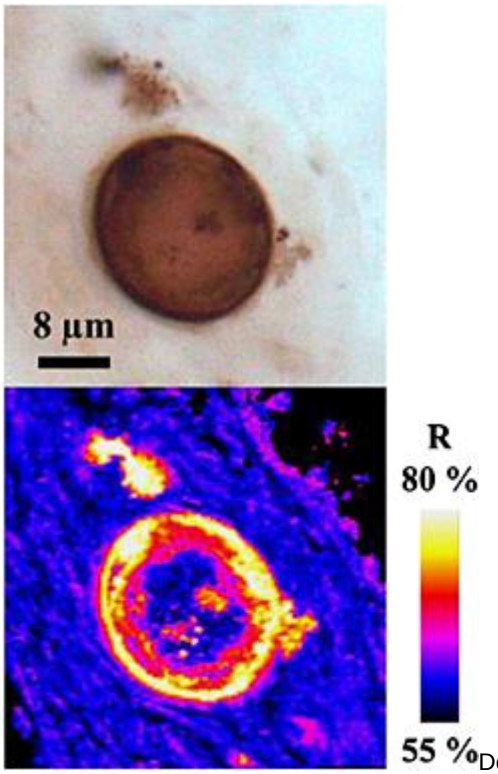

Demonstrating the biogenicity of carbonaceous matter is not possible simply using its Raman spectrum, but we show here that Raman mapping documents non-random distribution of variations in the intensity ratio R of the two main peaks of carbonaceous matter within 800-Ma-old microfossils. We conclude that these variations can be used as a proof of biogenicity. This discovery is of great interest and could help to detect potential fossilized microbial remains on Mars.

Internal diamond morphology: Raman imaging of metamorphic diamonds (pages 880–888)
Andrey V. Korsakov, Jan Toporski, Thomas Dieing, Jianyong Yang and Pavel S. Zelenovskiy
Article first published online: 17 JUN 2015 | DOI: 10.1002/jrs.4738

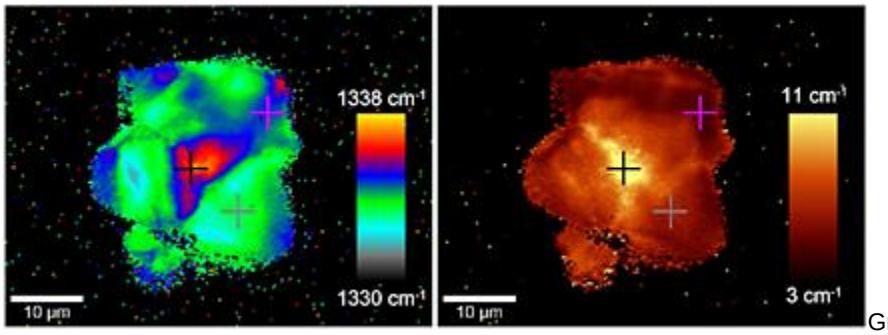

Growth history of metamorphic diamond crystals can be determined by detailed Raman imaging. The diamond shows a strong change in the position of the diamond Raman line and the width of this line. The broadening and upshift of main diamond band do not relate to residual strain in the inclusion–host system. A comparison of Raman imaging results with cathodoluminescence images reveals that the distribution of defects, which cause the cathodoluminescence of diamond crystals, can be traced by Raman imaging.

The role of intensity and instrument sensitivity in Raman mineral identification (pages 889–893)
P. R. Bartholomew, M. D. Dyar and J. B. Brady
Article first published online: 12 MAY 2015 | DOI: 10.1002/jrs.4707

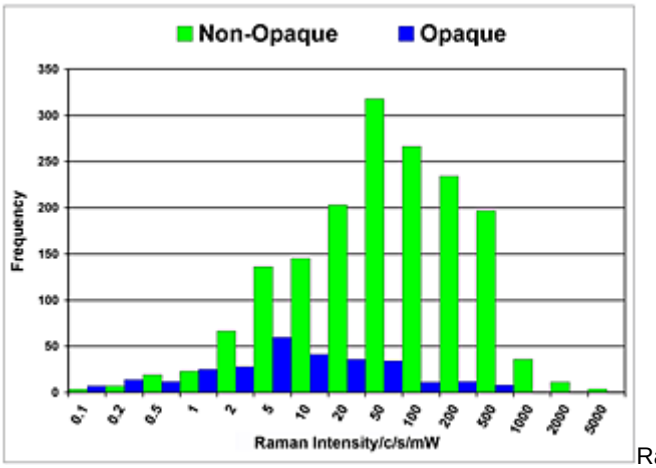

Raman spectroscopy could be a very effective tool for routine mineral identification if the Raman systematics for minerals, such as intensity variation, was better understood. A comparison of normalized Raman intensities of 7978 spectra from the RRUFF database shows that Raman intensities for minerals span four orders of magnitude, and opaque minerals generally have one order of magnitude lower intensity than non-opaque minerals.

Machine learning tools formineral recognition and classification from Raman spectroscopy (pages 894–903)
C. Carey, T. Boucher, S. Mahadevan, P. Bartholomew and M. D. Dyar
Article first published online: 10 AUG 2015 | DOI: 10.1002/jrs.4757

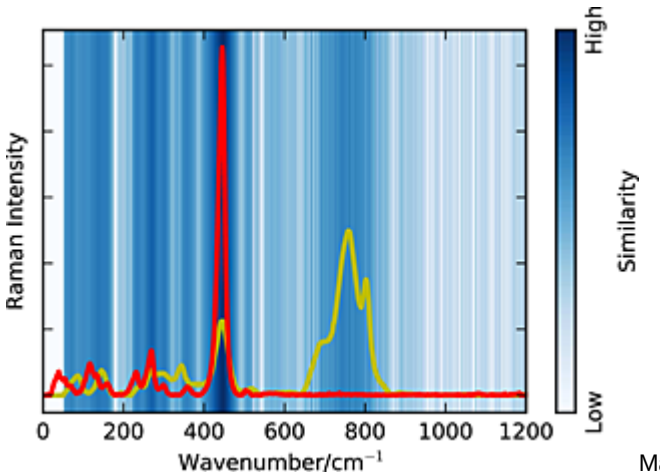

Machine learning techniques are applied to improve mineral identification using whole-spectrum analysis. Careful application of preprocessing steps, similarity scoring functions, and classification algorithms yields performance improvements on a real-world task.

***In situ* ambient and high-temperature Raman spectroscopic studies of nyerereite $(Na,K)_2Ca(CO_3)_2$: can hexagonal zemkorite be stable at earth-surface conditions? (pages 904–912)**
A. V. Golovin, A. V. Korsakov and A. N. Zaitsev
Article first published online: 27 JUL 2015 | DOI: 10.1002/jrs.4756

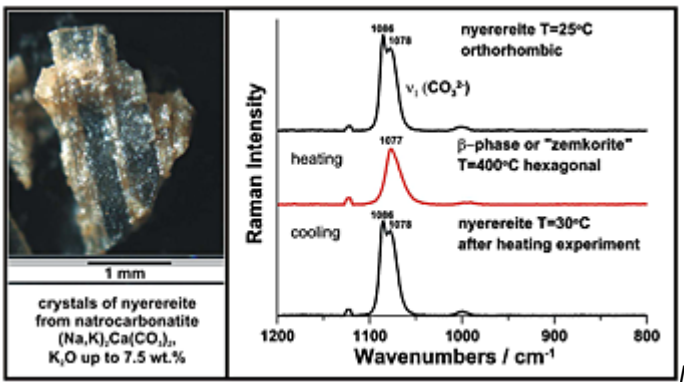

In situ ambient and high-temperature Raman spectroscopic study of natural carbonate nyerereite reveals that (1) there are the significant differences in Raman spectra of synthesized hexagonal 'zemkorite' and orthorhombic nyerereite, (2) zemkorite is non-quenchable and transformed to nyerereite at ambient condition and (3) presence of K_2O in synthesized zemkorite did not stabilize the structure during the quenching. We do not expect to find hexagonal zemkorite in natural magmatic, metasomatic or hydrothermal rocks exposed at the Earth surface.

Darwin impact glass study by Raman spectroscopy in combination with other spectroscopic techniques (pages 913–919)

L. Gomez-Nubla, J. Aramendia, A. Alonso-Olazabal, S. Fdez-Ortiz de Vallejuelo, K. Castro, L. A. Ortega, M. C. Zuluaga, X. Murelaga and J. M. Madariaga

Article first published online: 24 MAY 2015 | DOI: 10.1002/jrs.4700

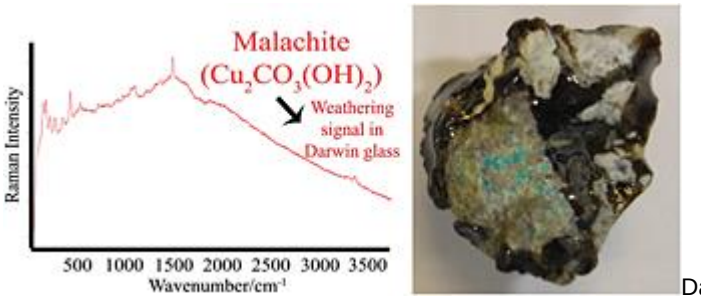

Darwin glasses are impact glasses found in west Tasmania and formed 800 000 years ago. Raman spectroscopy has been used to characterise the materials' molecular structure and obtain a clearer understanding of the formation of these unique glasses. Moreover, interesting results have been found about the weathering process that some of the analysed specimens has experienced.

Raman and infrared spectroscopic characterization of the arsenate-bearing mineral tangdanite– and in comparison with the discredited mineral clinotyrolite (pages 920–926)

Ray L. Frost, Ricardo Scholz and Andrés López

Article first published online: 15 APR 2015 | DOI: 10.1002/jrs.4691

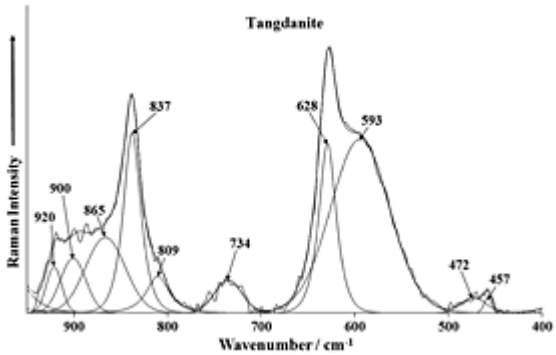

The mixed anion mineral tangdanite $Ca_2Cu_9(AsO_4)_4(SO_4)_{0.5}(OH)_9{\cdot}9H_2O$ has been studied using a combination of SEM, EDX, and Raman and infrared spectroscopy.

Evaluation of portable Raman instruments with 532 and 785-nm excitation for identification of zeolites and beryllium containing silicates (pages 927–932)

Jan Jehlička and Peter Vandenabeele

Article first published online: 10 JUN 2015 | DOI: 10.1002/jrs.4732

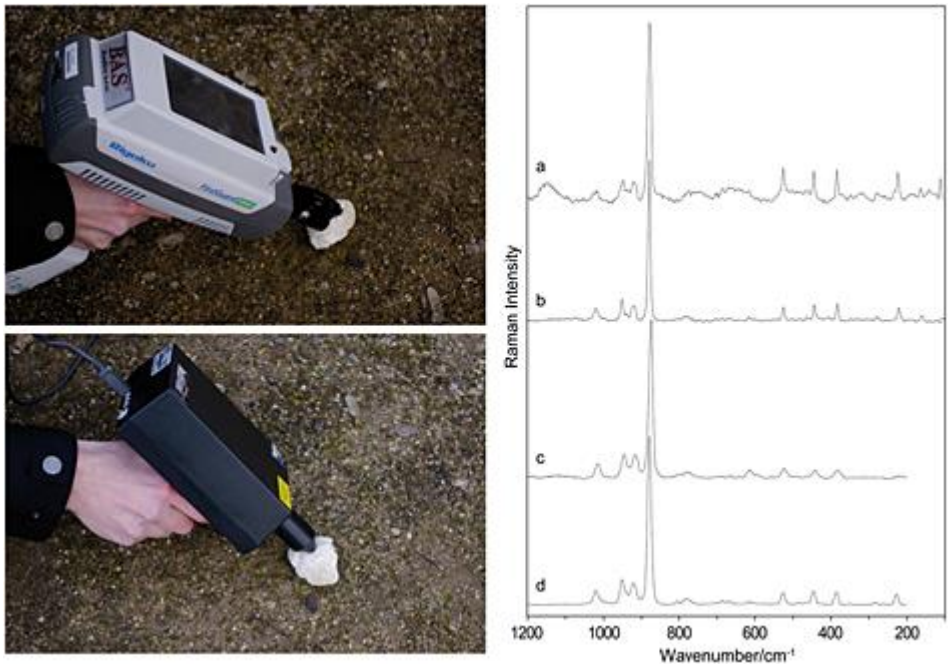

In this paper we present Raman spectra of zeolites and beryllium-containing silicates obtained outdoors on collection samples by handheld and portable dual instruments with 532/785-nm excitation. Near-infrared excitation can be recommended for robust identification of these minerals.

Raman spectra of Ni–Mg kerolite: effect of Ni–Mg substitution on O–H stretching vibrations (pages 933–940)

Michel Cathelineau, Marie-Camille Caumon, Frédéric Massei, David Brie and Matthieu Harlaux

Article first published online: 18 JUN 2015 | DOI: 10.1002/jrs.4746

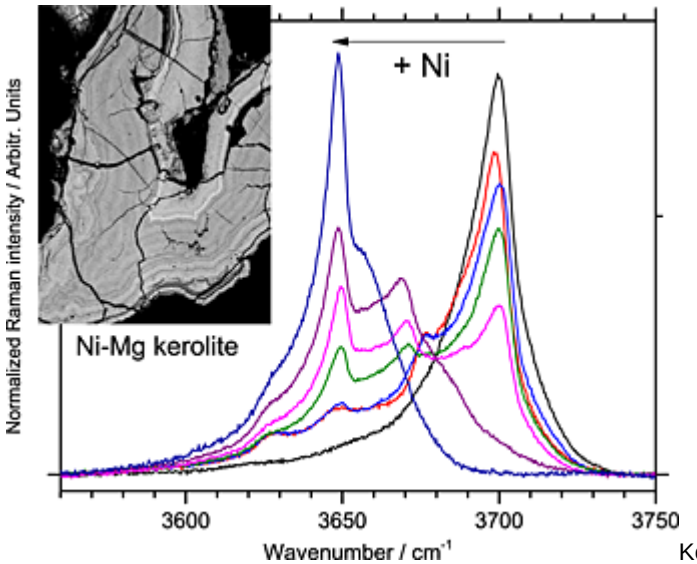

Key findings

Raman OH stretching vibrations in the talc-like mineral Ni–Mg kerolite are used to go further in the understanding of its crystal chemistry. The study is based on samples covering the whole substitution range of Mg by Ni with constant crystal chemistry, features and interlayer spacing, and no mixed-layering and on a chemometrics analysis of the Raman spectra. The heterogeneous distribution of Mg and Ni in the octahedral sheet is demonstrated, along

with the complexity of hydroxyl site geometry in comparison with talc.

Study of the spectro-chemical signatures of cobalt–manganese layered oxides (asbolane–lithiophorite and their intermediates) by Raman spectroscopy (pages 941–952)

C. Burlet and Y. Vanbrabant

Article first published online: 27 JUL 2015 | DOI: 10.1002/jrs.4755

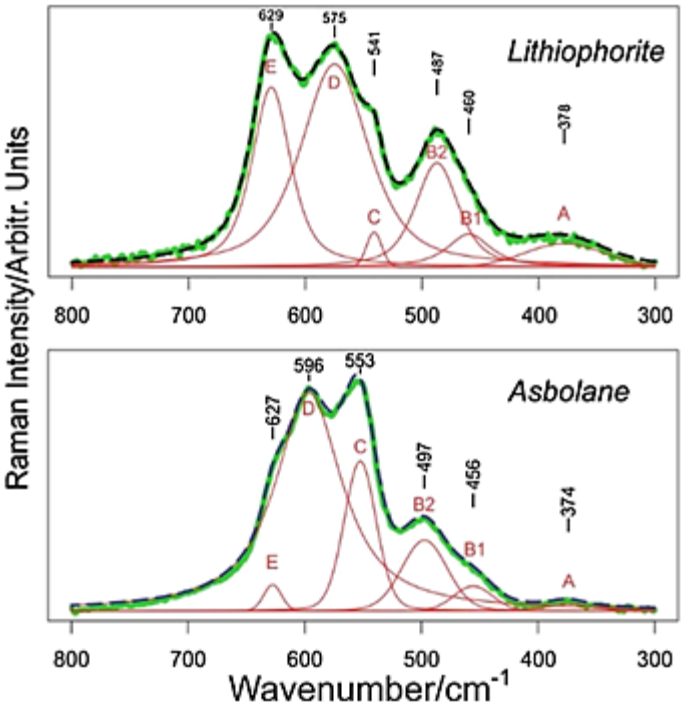

- - Raman microspectroscopy is applied to investigate two manganese oxide phases: lithiophorite [$(Al,Li)Mn^{4+}O_2(OH)_2$] and asbolane [$(Ni,Co)_xMn^{4+}(O,OH)_4 \cdot nH_2O$], along with their intermediates.
- - We show that Raman micro spectroscopy is useful to the investigation of those phases, but they require to be tested in very low laser power conditions to avoid sample degradation.
- - We assess the impact of their highly variable chemistry on their Raman peak positions, intensities and FWHM using a semi-systematic curve-fitting method profiled for these phases.

Micro-Raman mapping of the polymorphs of serpentine (pages 953–958)

J. R. Petriglieri, E. Salvioli-Mariani, L. Mantovani, M. Tribaudino, P. P. Lottici, C. Laporte-Magoni and D. Bersani

Article first published online: 14 APR 2015 | DOI: 10.1002/jrs.4695

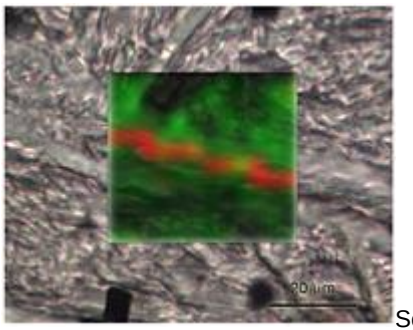

Serpentinites are rocks formed in large extent by minerals of the serpentine group: chrysotile, antigorite, lizardite, and polygonal serpentine. The identification of the main varieties of the serpentine group is of great interest for public health. Raman maps obtained in the OH region allow the discrimination of the four serpentine varieties. The identification of the different varieties of serpentine, at a

micrometric scale, directly on the sample, within their textural environment, provides a new level of detail in the study of serpentinization process.

Raman spectra of natural carbonaceous materials from a black shale formation (pages 959–963)
Tatyana N. Moroz, Victor A. Ponomarchuk, Sergei V. Goryainov, Nadezhda A. Palchik, Howell G. M. Edwards and Sergei M. Zhmodik
Article first published online: 26 AUG 2015 | DOI: 10.1002/jrs.4777

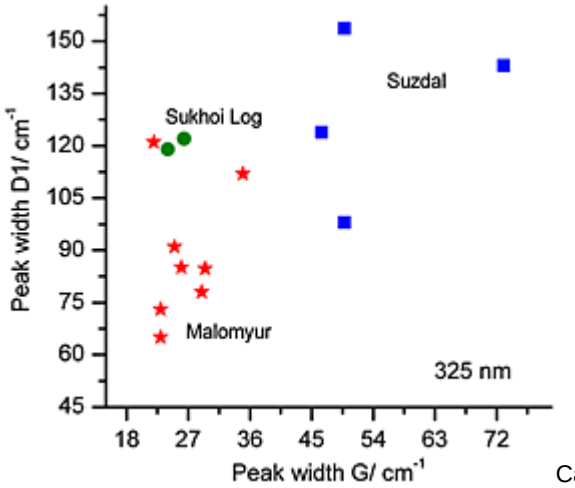

Carbonaceous materials in black-shale rocks from three gold-ore deposits located in Russia (Malomyur and Sukhoi Log) and Kazakhstan (Suzdal) have been investigated by micro-Raman spectroscopy using near-ultraviolet, visible and near-infrared excitations. Only laser excitation wavelength at 325 nm successfully yielded the Raman spectra for all samples. We show that the carbonaceous materials are substantially varied in their structural-ordering degree both in samples from the same deposit and, to a greater extent, in samples from the black-shale of different types.

Temperature-related changes of bioapatite based on hypermineralized dolphin's bulla (pages 964–968)
Zhen Li, Shipeng Wu and Chenglong Ye
Article first published online: 2 FEB 2015 | DOI: 10.1002/jrs.4653

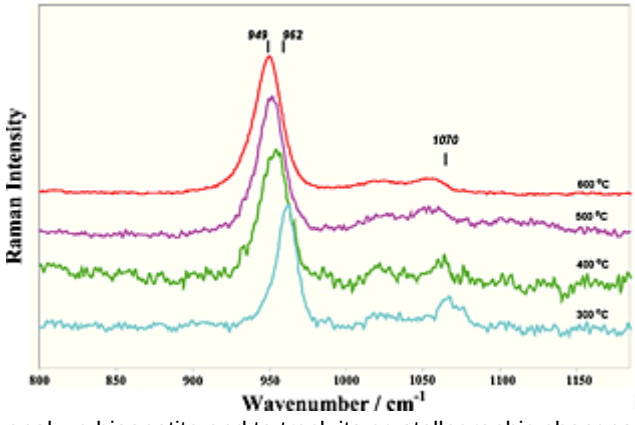

Micro-Raman spectroscopy is a powerful technique to analyze bioapatite and to track its crystallographic changes during heating. Decrystallization of bioapatite starts at 300 °C, and recrystallization begins at 600 °C. From 300 °C to 600 °C, a gradual process of phase change advances, and carbonate in bioapatite is depleted at ~500 °C. A new phase-hydroxylapatite will be initially formed at 700 °C, and then its crystallinity was significantly improved at 900 °C.

Raman spectra of water in fluid inclusions: I. Effect of host mineral birefringence on salinity measurement (pages 969–976)
Marie-Camille Caumon, Alexandre Tarantola and Régine Mosser-Ruck
Article first published online: 12 MAY 2015 | DOI: 10.1002/jrs.4708

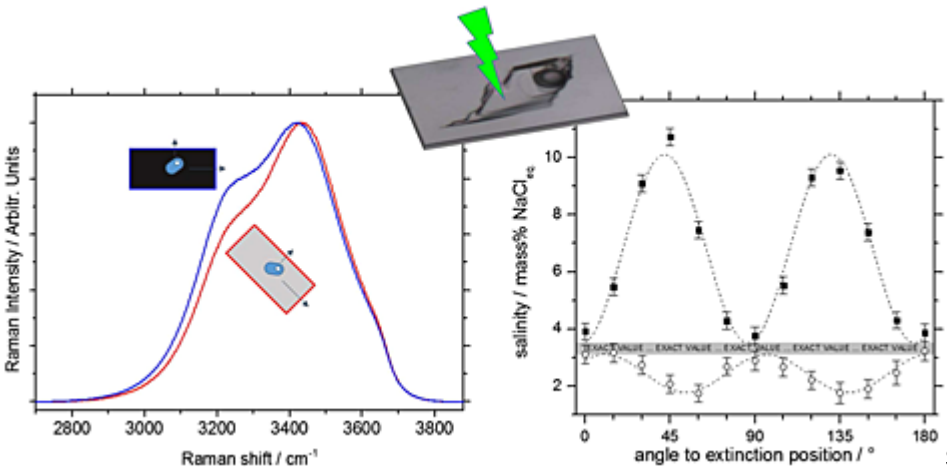

Salinity of aqueous fluid inclusions can be determined by Raman. The comparison with microthermometry highlighted that any birefringent mineral may affect salinity because of mineral birefringence, and of the polarization properties of the OH stretching vibration band of liquid water and of the spectrometers gratings. A good knowledge of the polarization properties of the optical devices of the Raman spectrometer and a correct positioning of the sample thus result in salinity measurements with the same accuracy as classic microthermometry.

Raman spectra of water in fluid inclusions: II. Effect of negative pressure on salinity measurement (pages 977–982)

Alexandre Tarantola and Marie-Camille Caumon

Article first published online: 17 MAR 2015 | DOI: 10.1002/jrs.4668

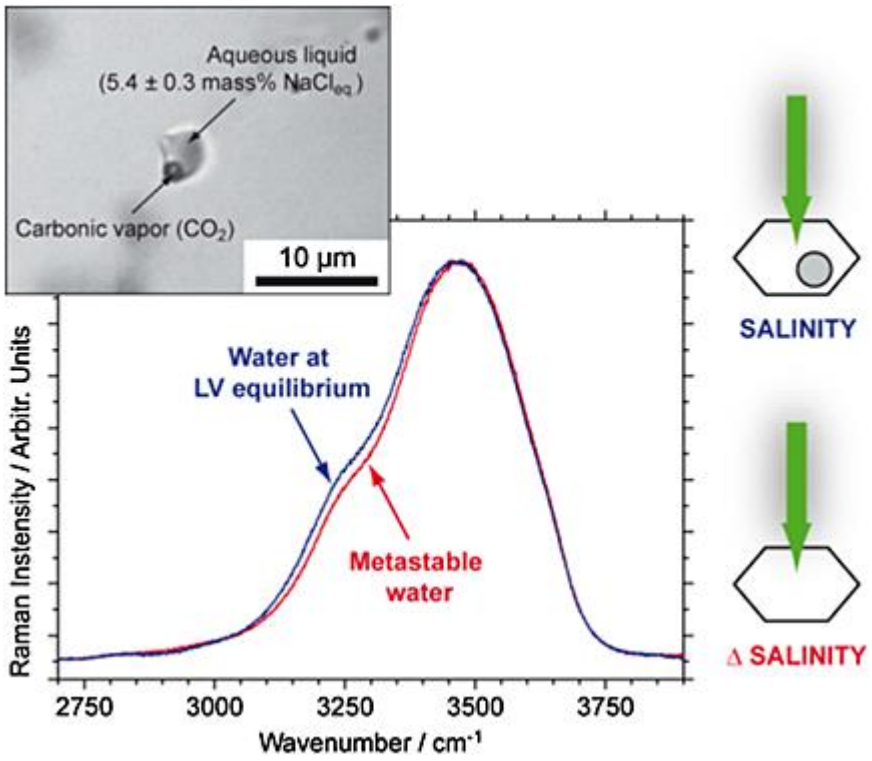

- The Raman signal of water is a function of salinity
- The salinity of natural fluid inclusions is measured in stable and metastable equilibrium
- The value of salinity of metastable fluid inclusions measured by Raman spectroscopy is a function of

negative pressure

Hydrogen in silicate melt inclusions in quartz from granite detected with Raman spectroscopy (pages 983–986)

Jiankang Li and I-Ming Chou

Article first published online: 26 JAN 2015 | DOI: 10.1002/jrs.4644

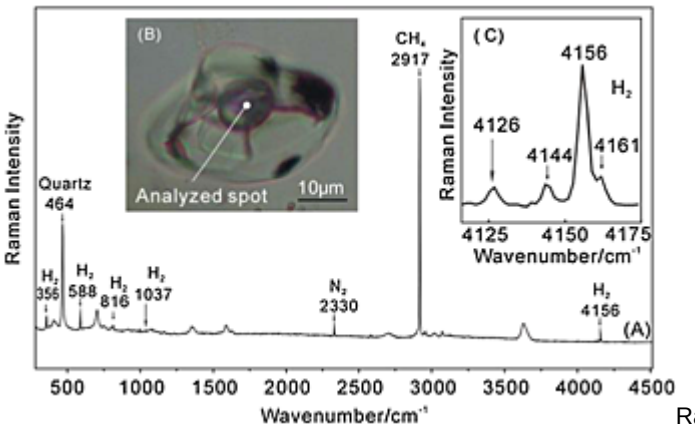

Raman spectroscopic analyses of silicate melt inclusions (SMIs) in quartz, from granite of Jiajika lithium pegmatite deposit in China, revealed the existence of H_2 in the vapor phase; the mechanisms for the formation of H_2 are unknown, and further research is needed.

Calibration of Raman shifts of cyclohexane for quantitative analyses of methane density in natural and synthetic fluid inclusions (pages 987–988)

I-Ming Chou

Article first published online: 16 JAN 2015 | DOI: 10.1002/jrs.4643

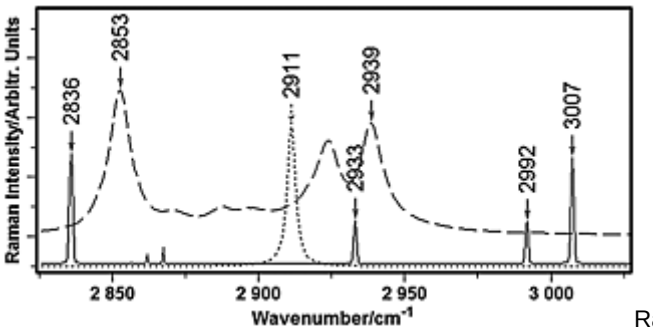

Raman spectra for cyclohexane (dashed line), methane vapor (dotted line), and Ne emission lines and the one Ne–He line at 2992 cm^{-1} (solid line). The two marked peak positions for cyclohexane, calibrated based on the Ne emission lines, were used to determine the CH_4 v_1 peak position for CH_4 density determination.

Nondestructive investigation on the 17-18th centuries Sicilian jewelry collection at the Messina regional museum using mobile Raman equipment (pages 989–995)

G. Barone, D. Bersani, J. Jehlička, P. P. Lottici, P. Mazzoleni, S. Raneri, P. Vandenabeele, C. Di Giacomo and G. Larinà

Article first published online: 24 FEB 2015 | DOI: 10.1002/jrs.4649

In this work, a handheld Raman spectrometer was used to analyze 15 jewels (necklaces, earrings, rings, brooches, hairclips, and precious belts) from the relevant jewelry collection preserved in the Regional Museum of Messina. The composition of the most important and interesting gems has been identified. For many jewels, the identification was consistent with the historical attribution, whereas in different cases, the obtained results revealed the use of natural and artificial simulants.

Investigating the firing protocol of Athenian pottery production: A Raman study of replicate and ancient sherds (pages 996–1002)
Ilaria Cianchetta, Jeff Maish, David Saunders, Marc Walton, Apurva Mehta, Brendan Foran and Karen Trentelman
Article first published online: 25 FEB 2015 | DOI: 10.1002/jrs.4662

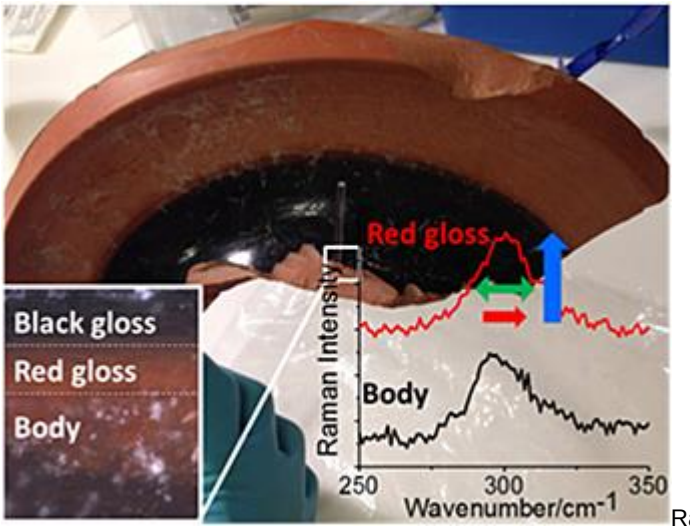

Raman spectroscopy was used to identify the mineralogical phases present in a fragment from an ancient Greek vessel. The shape and position of the E_g mode in hematite provided a measure of the temperatures at which the minerals were formed. The results suggest that the ancient vessel was produced using at least two separate firings: a high temperature firing under oxidizing conditions to create the underlying red glossy layer, followed by a three-step firing to create the surface black gloss decoration.

Raman spectroscopy for the investigation of carbon-based black pigments (pages 1003–1015)
Alessia Coccato, Jan Jehlicka, Luc Moens and Peter Vandenabeele
Article first published online: 4 JUN 2015 | DOI: 10.1002/jrs.4715

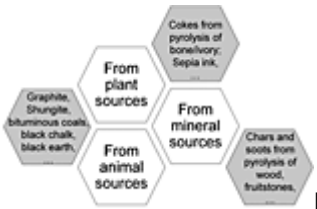

In comparison to graphite, disordered carbonaceous materials used as pigments in works of art show:

- Band shifts,

- Increase in bandwidth,
- The appearance of disorder related (D) bands.

These factors can be informative on the source and origin of the used pigment.

Micro-Raman analysis of pigments from hunter–gatherer archaeological sites of North Patagonia (Argentina) (pages 1016–1024)

Anastasia Rousaki, Cristina Bellelli, Mariana Carballido Calatayud, Veronica Aldazabal, Graciella Custo, Luc Moens, Peter Vandenabeele and C. Vázquez

Article first published online: 8 JUN 2015 | DOI: 10.1002/jrs.4723

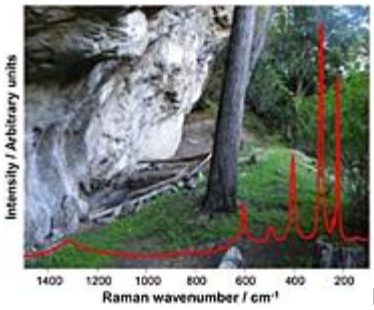

In Northern Patagonia, 30 samples from two hunter-gatherer regions (Traful Lake and Manso River areas) were investigated by micro-Raman spectroscopy, complemented with X-ray fluorescence. Micro-Raman analysis in rock art fragments, grinding tools, shell, raw pigment material, and painted ceramics and beads revealed haematite (Fe_2O_3) as the red chromophore. The identification of associated minerals and silicates in the mixtures pointed to the use of a clay-like material (ochre), rather than pure haematite.

Experimental determination of CO_2 diffusion coefficient in aqueous solutions under pressure at room temperature via Raman spectroscopy: impact of salinity (NaCl) (pages 1025–1032)

Clément Belgodere, Jean Dubessy, Denis Vautrin, Marie-Camille Caumon, Jérôme Sterpenich, Jacques Pironon, Pascal Robert, Aurélien Randi and Jean-Pierre Birat

Article first published online: 25 JUN 2015 | DOI: 10.1002/jrs.4742

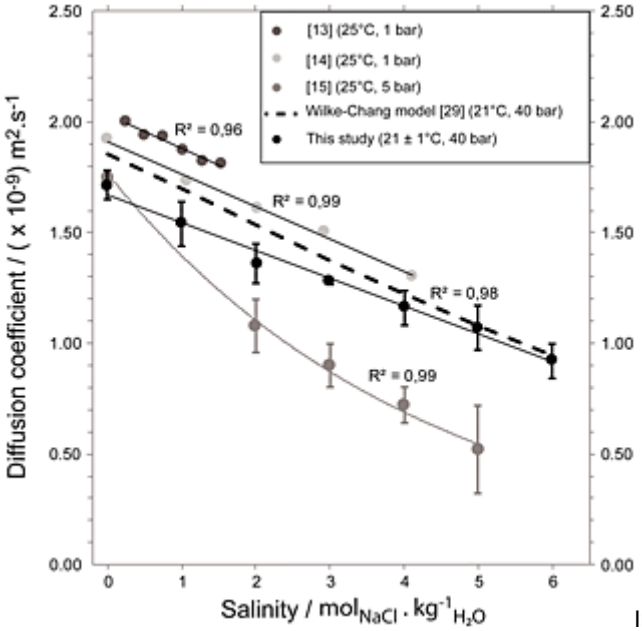

In this work, the diffusion coefficients of dissolved CO_2 were determined using *in situ* Raman microspectrometry in Fused Silica Capillaries in a range of salinity from 0.0 to 6.0 $mol_{NaCl}.kg^{-1}{}_{H2O}$. The diffusion coefficient of CO_2 dissolved in pure water at 21 ± 1 °C and 40 bar is $1.71 \times 10^{-9} \pm 0.06\ m^2.s^{-1}$. In the same conditions of pressure and temperature, the diffusion coefficient of dissolved CO_2 decreases (divided by two) with salinity increase from 0.0 to 6.0 $mol_{NaCl}.kg^{-1}{}_{H2O}$.

Short communication

Raman spectroscopy of pyrite in marble from Chillagoe, Queensland (pages 1033–1036)

Andrés López and Ray L. Frost

Article first published online: 29 APR 2015 | DOI: 10.1002/jrs.4699

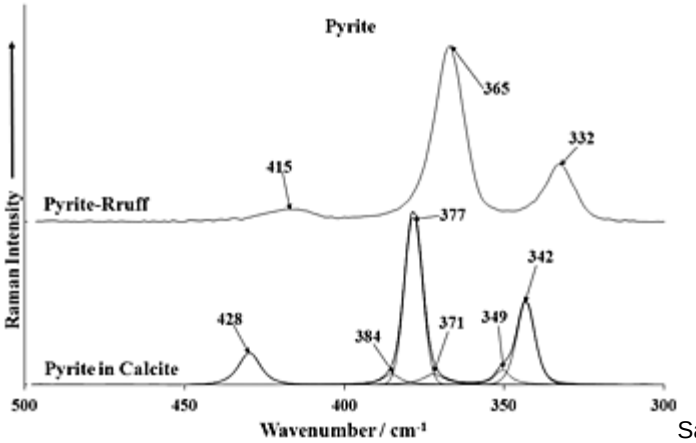

Samples of marble from Chillagoe, North Queensland have been analysed using electron microscopy with energy dispersive X-ray spectroscopy (EDS) and Raman spectroscopy. Raman spectroscopy identifies the presence of pyrite in black marble.